

MICROBIOLOGY

Bacterial spore germination receptors are nutrient-gated ion channels

Yongqiang Gao^{1†}, Jeremy D. Amon^{1†‡}, Lior Artzi^{1‡§}, Fernando H. Ramírez-Guadiana¹, Kelly P. Brock^{2¶}, Joshua C. Cofsky³, Deborah S. Marks², Andrew C. Kruse³, David Z. Rudner^{1*}

Bacterial spores resist antibiotics and sterilization and can remain metabolically inactive for decades, but they can rapidly germinate and resume growth in response to nutrients. Broadly conserved receptors embedded in the spore membrane detect nutrients, but how spores transduce these signals remains unclear. Here, we found that these receptors form oligomeric membrane channels. Mutations predicted to widen the channel initiated germination in the absence of nutrients, whereas those that narrow it prevented ion release and germination in response to nutrients. Expressing receptors with widened channels during vegetative growth caused loss of membrane potential and cell death, whereas the addition of germinants to cells expressing wild-type receptors triggered membrane depolarization. Therefore, germinant receptors act as nutrient-gated ion channels such that ion release initiates exit from dormancy.

Bacteria in the orders *Bacillales* and *Clostridiales* cause more than a million infections each year and are responsible for huge monetary losses to the food industry (1, 2). These bacteria resist antibiotics and sterilization by entering a highly durable spore state (3). Spores are metabolically inactive and can remain dormant for decades. However, upon exposure to nutrients, spores rapidly resume growth and can cause food spoilage, food-borne illness, or life-threatening disease. This exit from dormancy, called germination, is a key target in combating these pathogens. The germination program of most spore-forming bacteria involves a common series of chemical steps and a small set of broadly conserved factors (4, 5). GerA family receptors embedded in the spore membrane are required for sensing amino acids, sugars, and/or nucleosides. Nutrient detection leads to the release of mono- and divalent cations from the spore core, which is rapidly followed by the expulsion of large stores of dipicolinic acid (DPA) through the SpoVA transport complex (6, 7). DPA release activates cell wall hydrolases that degrade the specialized peptidoglycan that encases the spore, allowing core rehydration, macromolecular synthesis, and resumption of growth. The prototypical germinant receptor, GerA, in *Bacillus subtilis* is composed of three broadly conserved subunits: GerAA, GerAB, and GerAC (8). GerAB is responsible for L-alanine

recognition, and genetic evidence suggests that nutrient detection by GerAB is communicated to the GerAA subunit (9, 10). How this signal triggers germination and exit from dormancy remains unclear (11).

To elucidate the germination process further, we examined the communication between GerA and the DPA transporter SpoVA. We reasoned that if GerA communicates with SpoVA through a protein-protein contact, then germination signal transduction would be broken if SpoVA were substituted with a homolog that was unable to maintain this contact. We expressed the *Bacillus cereus* *spoVA* operon (*spoVA1*) in *B. subtilis* with the expectation that the heterologous transporter (~70% identical; fig. S1A) would not be activated by the *B. subtilis* germination signal transduction pathway. Instead, *B. subtilis* spores harboring the SpoVA1 transporter and lacking the native *spoVA* locus released DPA and germinated in response to L-alanine in a manner similar to wild-type (Fig. 1A and figs. S2 to S4). Similar results were obtained with a different *B. cereus* *spoVA* locus (*spoVA2*, ~56% identical) and the *Clostridiodes difficile* *spoVA* operon (~46% identical) (Fig. 1A and figs. S1 to S4). *C. difficile* belongs to the small subset of spore formers that lacks GerA-family receptors (8, 12). These findings suggested that activation of SpoVA by GerA-family receptors is not mediated by protein-protein interactions and instead involves some chemical or physical change to the spore. To further test this idea, we performed a reciprocal experiment in which we expressed the *Bacillus megaterium* GerA-family receptor GerUV (fig. S1B) (13) in a *B. subtilis* strain lacking all of its native germinant receptors. These spores activated DPA release and germinated in response to GerUV's cognate germinants D-glucose, L-leucine, L-proline, and K⁺, but not in response to L-alanine (Fig. 1B and fig. S3).

The GerA complex is predicted to oligomerize into a membrane channel

The release of cations from the spore core is the first measurable event during germination, but the molecular basis for ion release and its role in exit from dormancy have been unclear (14, 15). On the basis of the cross-species complementation results described above, we hypothesized that GerA-family receptors trigger DPA export and exit from dormancy by releasing cations. GerAA and GerAB are polytopic membrane proteins and GerAC is a lipoprotein (4); a conserved set of glycine residues in transmembrane (TM) helix 3 in GerAA potentially indicated that these proteins might act as ion channels (Fig. 2A). Conserved glycine patches have been observed in the luminal helices of other ion channels, where they facilitate tight oligomeric packing (16). Accordingly, we investigated whether GerAA could multimerize using AlphaFold-Multimer (17–19). Indeed, AlphaFold predicted that GerAA could form a high-confidence pentamer with a membrane channel formed by TM helix 3 (Fig. 2B and fig. S5). Separately, AlphaFold also predicted that GerAC could form a pentamer (fig. S5C) and that the GerAA-GerAB-GerAC trimer could dimerize with a packing angle of ~69°, consistent with a pentameric complex (fig. S6). GerAA-GerAB-GerAC trimers could be superimposed upon all five protomers of the GerAA and GerAC pentamers without clashes (Fig. 2D and figs. S7 and S8). Furthermore, the ligand-binding pockets in the GerAB subunits were accessible to exogenous nutrients in the fully assembled complex (fig. S7C). All AlphaFold models were supported by low interresidue distance errors [predicted template modeling score (pTM) > 0.75] and strong per-residue accuracy estimates [predicted local distance difference test (pLDDT) > 85] (fig. S5). Thus, our modeling suggests that the GerA complex consists of a pentameric arrangement of heterotrimers (15 subunits total) that form a transmembrane channel.

Further support for this oligomeric model comes from evolutionary co-variation analysis (20) in which directly interacting amino acids tend to co-evolve and evolutionarily coupled (EC) residue pairs are generally close to each other in tertiary structure. Several high-confidence EC residue pairs within GerAA (Fig. 2C) and GerAC (fig. S9) were distant from each other within individual protomers but could be fully explained by intermolecular contacts in the oligomeric model (Fig. 2C and fig. S9, orange circles). Similarly, several EC residue pairs between the GerAA and GerAB subunits and between the GerAB and GerAC subunits were not satisfied by the predicted GerAA-GerAB-GerAC trimer but could be explained by intermolecular contacts in the predicted pentamer of trimers (fig. S9). All detected EC residue pairs within GerAB appeared to be

¹Department of Microbiology, Harvard Medical School, Boston, MA 02115, USA. ²Department of Biological Chemistry and Molecular Pharmacology, Harvard Medical School, Boston, MA 02115, USA. ³Department of Systems Biology, Harvard Medical School, Boston, MA 02115, USA.

*Corresponding author. Email: rudner@hms.harvard.edu

†These authors contributed equally to this work.

‡Present Address: Moderna Genomics, Cambridge, MA 02139, USA.

§Present Address: Evolved By Nature, Medford, MA 02155, USA.

¶Present Address: Kernal Biologics, Cambridge, MA 02142, USA.



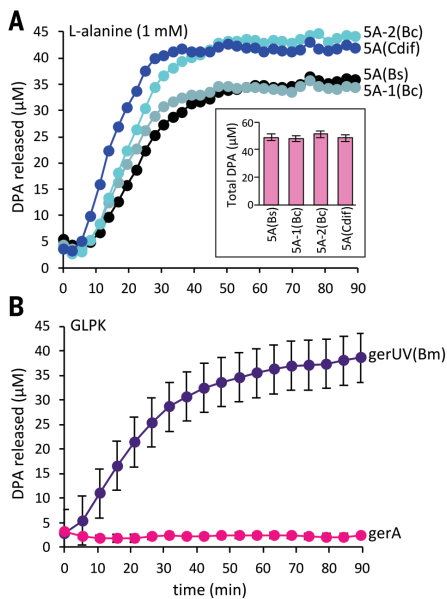


Fig. 1. Cross-species complementation of key germination factors. (A) *spoVA* loci from *B. cereus* and *C. difficile* support DPA release from *B. subtilis* spores in response to L-alanine. Purified spores of $\Delta spoVA$ mutant strains harboring an ectopic copy of the indicated *spoVA* (5A) locus from *B. subtilis* (Bs), *B. cereus* (Bc), or *C. difficile* (Cdif). Spores were mixed with 1 mM L-alanine, and DPA release was monitored over time. The insert shows total DPA content in purified spores. Representative data from one of three biological replicates are shown. The other two replicates can be found in fig. S2. (B) *B. subtilis* spores harboring the *gerUV* locus from *B. megaterium* germinate in response to D-glucose, L-leucine, L-proline, and K^+ (GLPK). Purified *B. subtilis* spores lacking all five endogenous germinant receptor loci ($\Delta 5$) and harboring the *gerUV* or *gerA* locus were incubated with GLPK (10 mM each), and DPA release was monitored over time. The data represent the average results from three biological replicates. Error bars indicate SDs. Similar results were obtained using a germination assay that monitors the drop in optical density as phase-bright spores transition to phase-dark (figs. S3 and S4).

intramolecular contacts (fig. S9), consistent with the observation that GerAB protomers did not contact each other in the predicted pentameric arrangement (Fig. 2D and fig. S7).

The predicted membrane channel formed by the GerAA pentamer is lined with hydrophilic residues, contains a stereotypical glycine patch, and has dimensions similar to those of previously characterized ligand-gated ion channels (Fig. 2E and fig. S10) (16, 21, 22). Furthermore, acidic residues are enriched at the periphery of the channel, suggesting cation selectivity (fig. S10C). Pentameric ligand-gated ion channels constitute a large family of neurotransmitter receptors that includes the cation-selective nicotinic acetylcholine receptor and the anion-selective γ -aminobutyric acid (GABA) receptor (21). Al-

though evolutionarily unrelated, these neurotransmitter receptors and the GerAA oligomer share a common channel-forming structural motif comprising a three-helix bundle that, with symmetry, traces two concentric rings around the pore axis (Fig. 2F and fig. S10B) (23, 24).

GerA complexes function as membrane channels

The GerA structural prediction was bolstered by an unbiased genetic screen. The screen identified hyperactive *gerAA* alleles that constitutively trigger germination. We mutagenized *gerAA* by polymerase chain reaction and screened for dominant mutants with defects in spore maturation (fig. S11A). The three strongest mutants identified caused premature germination and pervasive lysis during spore formation (Fig. 2G and fig. S11CD). The few unlysed spores had teardrop shapes, suggesting a severe defect in morphogenesis. All three mutants had amino acid substitutions in or adjacent to TM helix 3 (fig. S11B), one of which (V362A) was predicted to face directly into the lumen of the channel (Fig. 2F). In the context of the structural model, this conservative substitution would widen the channel and potentially maintain it in an open state. To test this, we separately substituted leucine 358 (fig. S11B), which is also predicted to be in TM helix 3 and face the lumen of the channel, with alanine. GerAA(L358A) similarly caused premature germination with teardrop-shaped spores (fig. S11CD). To investigate whether narrowing the channel would impair GerAA function, we substituted valine 362 with leucine. Upon exposure to L-alanine, spores harboring GerAA(V362L) were unable to release monovalent ions or DPA and its Ca^{2+} chelate and failed to rehydrate as assayed by optical density (Fig. 2H and figs. S12 and S13). We conclude that the V362L mutation fully impaired germination. The GerAA(V362L) protein was stable in spores and maintained the stability of GerAC (Fig. 2I and fig. S13C), suggesting that the mutant subunit assembled into germination complexes (10, 25). GerAA(V362L), like wild-type GerAA [GerAA(WT)], localized in clusters called germinosomes (26) in the spore membrane (Fig. 2J and fig. S13D), further suggesting that the mutant protein was properly assembled into germination receptor complexes but incapable of transducing nutrient signals. Leucine substitutions at two other positions in GerAA's TM helix 3 (Q354 and Q366) that were also predicted to face the lumen of the channel behaved similarly to GerAA(V362L) in all of the assays described above (figs. S12 and S13).

All A subunits in the GerA family that we analyzed using AlphaFold-Multimer were predicted to form pentameric membrane channels. The GerQA subunit encoded in the *B. cereus* *gerQ* operon (27) has an isoleucine at

position 363 in TM helix 3 that is analogous to valine 362 in GerAA (fig. S14A). Introduction of *gerQA*(I363A) into *B. cereus* caused premature germination during sporulation and a reduction in spore viability (Fig. 3K and fig. S14B). Thus, most GerA-family receptors, including those from pathogenic organisms, are likely to function as channels.

GerA complexes act as nutrient-gated ion channels

To investigate whether the GerA complex releases ions, we expressed GerAB and GerAC in exponentially growing *B. subtilis* cells and placed *gerAA*(WT) and *gerAA*(V362A) under the control of an isopropyl β -D-thiogalactopyranoside (IPTG)-regulated promoter. Cells expressing GerAA(V362A) were not viable (Fig. 3A and fig. S15). Loss of viability was GerAB and GerAC dependent (Fig. 3, A and B), consistent with the requirement of a fully assembled GerA complex for toxic activity. Similar results were obtained with the other constitutively active *gerAA* alleles (fig. S16). Inducible growth defects have been reported for mechanosensitive channel mutants that are locked in an open state (28, 29), suggesting that GerAA(V362A)-GerAB-GerAC complexes cause constitutive ion release. To investigate this possibility, we monitored the loss of membrane potential using the potentiometric fluorescent dye 3,3'-dipropylthiadicarbocyanine iodide [DiSC₃(5)] (30). Within 10 min after inducing *gerAA*(V362A), we detected a drop in DiSC₃(5) fluorescence, which decreased further over the next 30 min (Fig. 3C and fig. S17). Membrane permeability defects, assayed with propidium iodide, occurred ~80 min after *gerAA*(V362A) induction (Fig. 3C and fig. S17). We observed no membrane integrity defects or depolarization when GerAA(WT) was expressed with GerAB and GerAC nor when GerAA(V362A) was expressed in their absence (Fig. 3C and fig. S17). The addition of 50 mM L-alanine to cells expressing GerAA(WT), GerAB, and GerAC caused a 30% reduction in DiSC₃(5) fluorescence (Fig. 3, D and E, and fig. S18). No reduction was observed when equimolar concentrations of L-alanine and the germinant-competitive inhibitor D-alanine (31) were added together (fig. S18). Furthermore, L-alanine did not reduce membrane potential when added to cells expressing the channel-narrowing GerAA(V362L) mutant or a GerAB mutant (G25A) in the ligand-binding pocket that does not respond to L-alanine (Fig. 3, D and E, and figs. S18 to S20) (10). Thus, the GerA complex acts as a nutrient-gated ion channel.

GerAA multimerizes in vivo

We used our vegetative GerA expression system to investigate whether GerAA subunits multimerize in vivo. First, we performed immunoprecipitation experiments from detergent-

solubilized membranes derived from cells coexpressing functional GerAA-ProteinC (GerAA-ProC) and GerAA-FLAG fusions (fig. S21). Anti-ProC resin efficiently coprecipitated GerAA-ProC and GerAA-FLAG if GerAB and GerAC were also expressed (Fig. 3F), indicating that at least two GerAA subunits reside in these membrane complexes. In a complementary set of experiments, we generated functional fluorescent fusions to GerAA (fig. S21) that formed discrete fluorescent foci that depended on GerAB and GerAC (Fig. 3G and fig. S22). Increasing expression of GerAA-mYpet resulted in an increase in the number of foci rather than an increase in the fluorescence intensity of individual foci, suggesting that each focus is a discrete oligomeric complex rather than a nonspecific aggregate (fig. S23). Multimerization of GerAA *in vivo* was further supported by

experiments in sporulating cells expressing equivalent levels of GerAA(WT) and GerAA(V362L) (fig. S24A). The channel-blocking mutant was strongly dominant-negative for spore germination, suggesting that GerAA(V362L) assembles into complexes with GerAA(WT) and poisons their function (fig. S24). For comparison, the merodiploid spores were more severely impaired in DPA release and germination than spores with a *gerA4* allele that produced about eightfold lower levels of GerAA(WT) (fig. S24).

As a final *in vivo* test of the AlphaFold-predicted GerA oligomer, we engineered cysteine substitutions in GerAA at positions predicted to reside within 5 Å of each other in adjacent TM3 channel helices (fig. S25A). These variants were expressed in vegetative cells and then analyzed by immunoblot. We

observed two high-molecular-weight GerAA species of ~100 and 250 kDa, consistent with a dimer and a pentamer (Fig. 3H). Both species were observed in the absence of exogenous chemical cross-linking reagents and were stable in the presence of sodium dodecyl sulfate and β-mercaptoethanol, but not tributyl phosphine, as expected for disulfide bonds within TM segments (32) (fig. S24B). The 250-kDa species was only detected when both cysteines were present in GerAA and when coexpressed with GerAB and GerAC (Fig. 3H). Furthermore, species of identical sizes were observed when the cysteine-substituted GerAA variant was analyzed from dormant spores (Fig. 3H). Two additional species were detectable, albeit weakly, in the spore lysate that could represent GerAA trimers and tetramers resulting from incompletely oxidized pentamers.

Fig. 2. Evidence that GerAA forms a membrane channel.

(A) Predicted structure of the GerAA (red), GerAB (cyan), and GerAC (purple) trimers. Topology is based on protease accessibility studies of GerAC and GerAA (10, 38). TM3, the lumen-adjacent helix in GerAA, is labeled. **(B)** Predicted GerAA pentamer as viewed from outside the spore. Protomers are shown in dark and light gray and red. **(C)** EC residue pairs in GerAA are plotted as black circles. Intra-protomer (blue circles) and interprotomer (orange circles) residue pairs that are ≤5 Å apart in the predicted GerAA pentamer are shown. **(D)** Space-filling model of the predicted pentamer of trimers. **(E)** Predicted pore (light blue) in the GerAA pentamer. Only three GerAA protomers are shown for clarity. **(F)** Top view of the GerAA hexamer model showing the concentric TM rings surrounding the channel. V362 is highlighted. **(G)** Representative phase-contrast images of sporulated cultures of strains harboring a second copy of *gerAA*(WT) or *gerAA*(V362A). The strain harboring *gerAA*(V362L) lacks the native *gerAA* copy. Scale bar, 3 μm. Inset highlights the teardrop-shaped spores in the V362A mutant. **(H)** Purified spores that have GerAA(WT) (circles) or GerAA(V362L) (squares) as the sole copy of the GerAA subunit were mixed with 1 mM L-alanine, and the germination exudates were analyzed for K⁺, Ca²⁺, and DPA over time. **(I)** Immunoblots from lysates of the purified spores used in (H). GerAA(WT) and GerAA(V362L) are stable and stabilize GerAC-His, unlike spores lacking GerAA (ΔAA). SpoVAD controls were used for loading. **(J)** Representative fluorescence images of GerAA(WT)-green fluorescent protein (GFP) and GerAA(V362L)-GFP localization in spores. Both localize in germinosome foci. Scale bar, 3 μm. **(K)** Representative phase-contrast images of sporulated cultures of wild-type *B. cereus* and a merodiploid strain harboring *gerQA*(I363A). Sporulation efficiency of each strain is indicated on the bottom right. Scale bar, 2 μm. Representative data from one of at least three biological replicates are shown for (G), (H), (J), and (K) and from one of two biological replicates for (I).

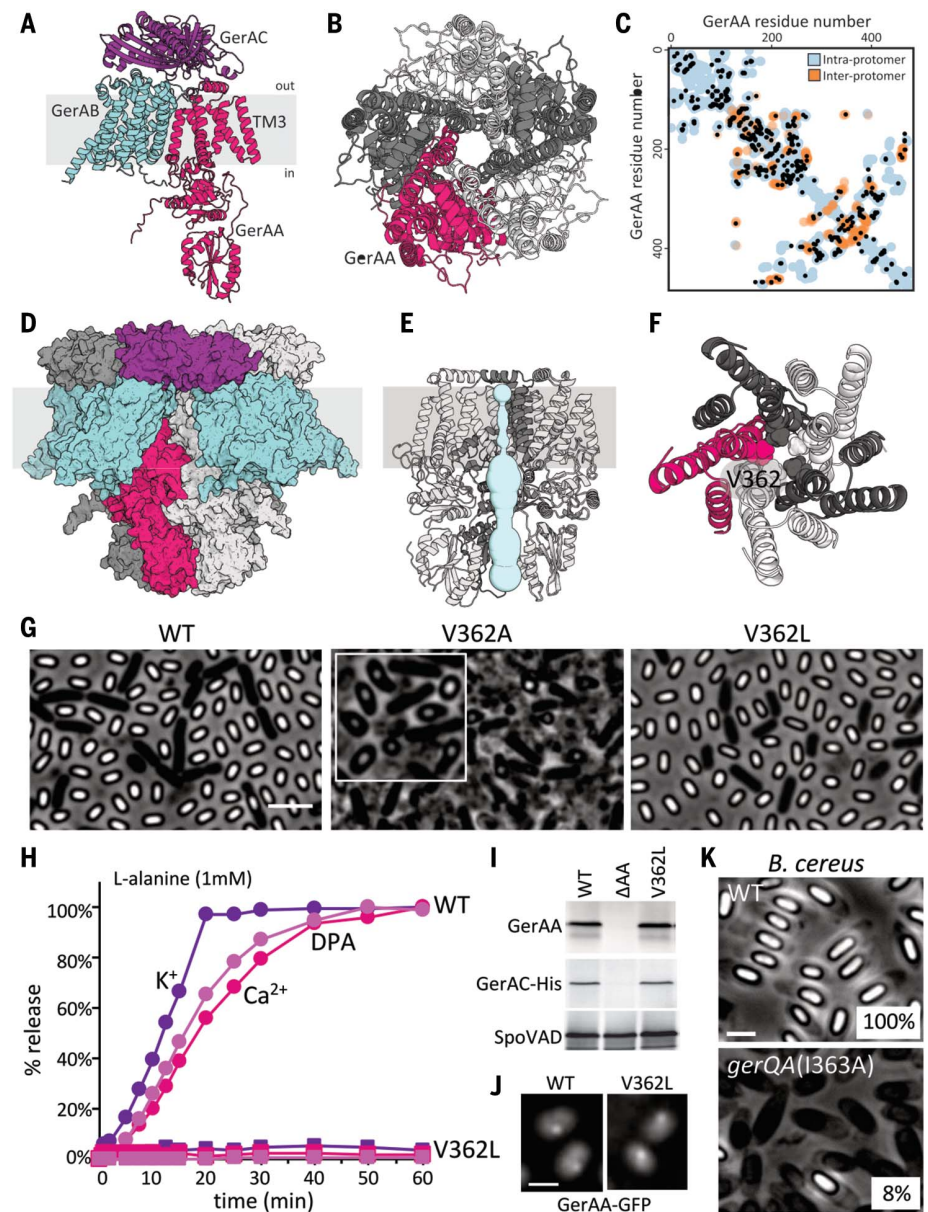


Fig. 3. The GerA complex behaves like a nutrient-gated ion channel when expressed in vegetatively growing cells.

(A) Serial dilutions of the indicated strains with IPTG-regulated *gerAA*(WT) and *gerAA*(V362A) alleles and constitutively expressed *gerAB* and *gerAC* (AC). (B) Immunoblot analysis of the strains in (A). GerAA(WT) and GerAA(V362A) were expressed at similar levels in the presence or absence of GerAB and GerAC. ScpB controls for loading.

(C) Representative fluorescence images of exponentially growing cultures of the indicated strains from (A). Time (in minutes) after IPTG addition is indicated. The top panels show fluorescence of the potentiometric dye DiSC₃(5). The lower panels show propidium iodide staining. The two fields are from the same culture but stained and imaged separately. Scale bar, 5 μm. (D) Representative DiSC₃(5) fluorescence images of exponentially growing cultures of the indicated strains 30 min after the addition of 50 mM L-alanine. *gerAA* and *gerAA*(V362L) are IPTG-regulated alleles, and *gerAB*, *gerAB*(G25A), and *gerAC* were expressed constitutively. (E) Quantitative analysis of DiSC₃(5) fluorescence intensity from the same strains and conditions as in (D). DiSC₃(5) fluorescence intensities were quantified from three biological replicates (>500 cells for each) and plotted in different colors. Triangles represent the median fluorescence intensity for each replicate, and red lines show the median values for all cells per strain. *P* values < 0.0001 (****) and not significant (ns) are indicated.

(F) Immunoblots of anti-ProC immuno-affinity purifications from detergent-solubilized membrane preparations of vegetatively growing *B. subtilis* cells expressing the indicated proteins. Load (L) and elution (Elu) are shown. GerAA-FLAG copurifies with GerAA-ProC if GerAB and GerAC are coexpressed. The membrane protein EzrA serves as a negative control. (G) Representative fluorescence images of vegetative cells expressing GerAA-GFP in the presence and absence of GerAB and GerAC. (H) Immunoblots of vegetative cells expressing cysteine-substituted GerAA variants in the presence or absence of GerAB and GerAC. GerAA(V359C G361C) produces disulfide species (red asterisks) with sizes of dimer and pentamer (left). Wall controls were used for loading. GerAA species of similar size were also detected from spore lysates (right). Two additional species were detected. SleB controls were used for loading. Representative data from one of at least three biological replicates are shown for (A), (C) to (E), (G), and (H). (B) and (F) are from one of two biological replicates.

(A) Serial dilutions of the indicated strains with IPTG-regulated *gerAA*(WT) and *gerAA*(V362A) alleles and constitutively expressed *gerAB* and *gerAC* (AC). (B) Immunoblot analysis of the strains in (A). GerAA(WT) and GerAA(V362A) were expressed at similar levels in the presence or absence of GerAB and GerAC. ScpB controls for loading.

(C) Representative fluorescence images of exponentially growing cultures of the indicated strains from (A). Time (in minutes) after IPTG addition is indicated. The top panels show fluorescence of the potentiometric dye DiSC₃(5). The lower panels show propidium iodide staining. The two fields are from the same culture but stained and imaged separately. Scale bar, 5 μm. (D) Representative DiSC₃(5) fluorescence images of exponentially growing cultures of the indicated strains 30 min after the addition of 50 mM L-alanine. *gerAA* and *gerAA*(V362L) are IPTG-regulated alleles, and *gerAB*, *gerAB*(G25A), and *gerAC* were expressed constitutively. (E) Quantitative analysis of DiSC₃(5) fluorescence intensity from the same strains and conditions as in (D). DiSC₃(5) fluorescence intensities were quantified from three biological replicates (>500 cells for each) and plotted in different colors. Triangles represent the median fluorescence intensity for each replicate, and red lines show the median values for all cells per strain. *P* values < 0.0001 (****) and not significant (ns) are indicated.

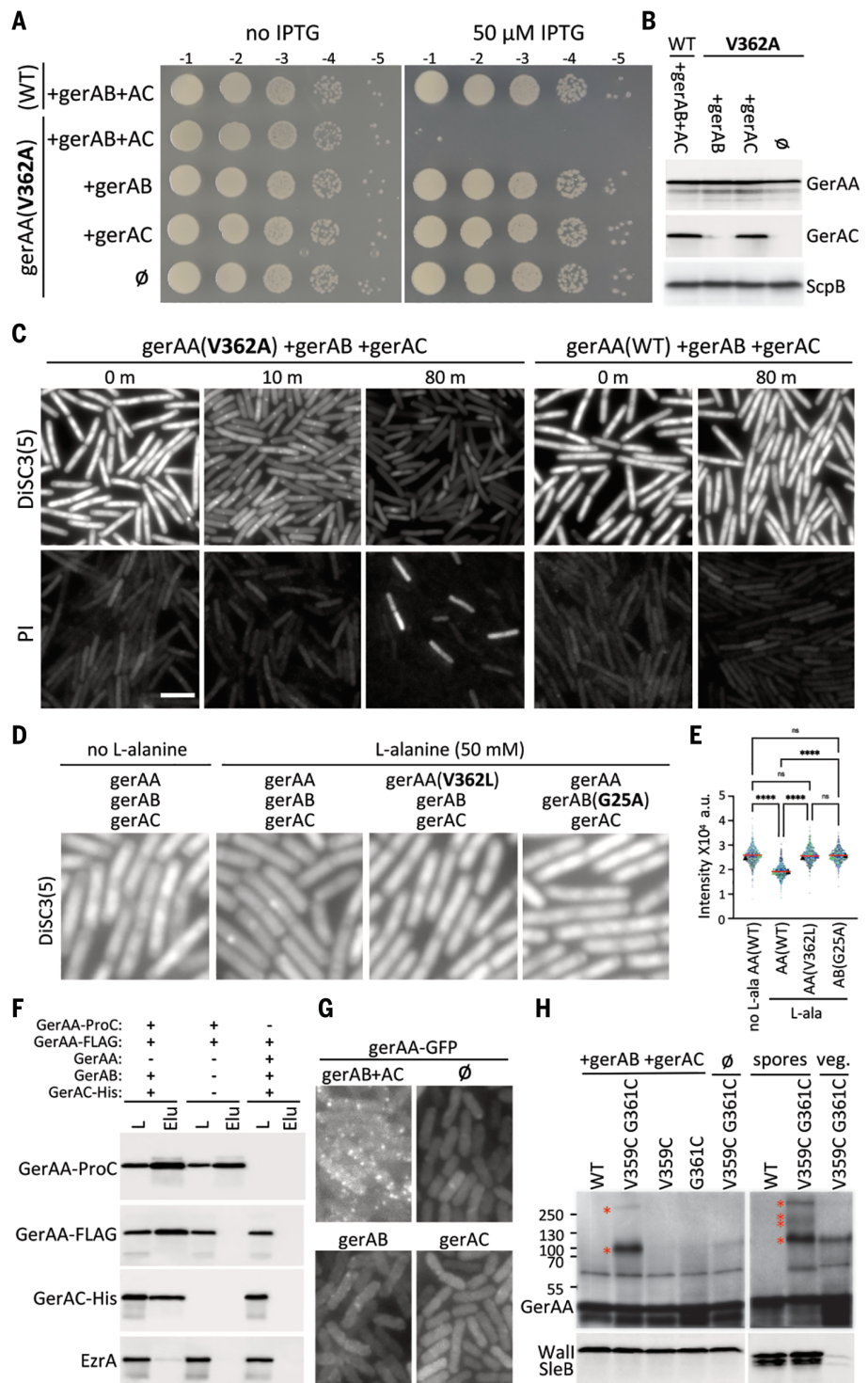
(F) Immunoblots of anti-ProC immuno-affinity purifications from detergent-solubilized membrane preparations of vegetatively growing *B. subtilis* cells expressing the indicated proteins. Load (L) and elution (Elu) are shown. GerAA-FLAG copurifies with GerAA-ProC if GerAB and GerAC are coexpressed. The membrane protein EzrA serves as a negative control. (G) Representative fluorescence images of vegetative cells expressing GerAA-GFP in the presence and absence of GerAB and GerAC. (H) Immunoblots of vegetative cells expressing cysteine-substituted GerAA variants in the presence or absence of GerAB and GerAC. GerAA(V359C G361C) produces disulfide species (red asterisks) with sizes of dimer and pentamer (left). Wall controls were used for loading. GerAA species of similar size were also detected from spore lysates (right). Two additional species were detected. SleB controls were used for loading. Representative data from one of at least three biological replicates are shown for (A), (C) to (E), (G), and (H). (B) and (F) are from one of two biological replicates.

(A) Serial dilutions of the indicated strains with IPTG-regulated *gerAA*(WT) and *gerAA*(V362A) alleles and constitutively expressed *gerAB* and *gerAC* (AC). (B) Immunoblot analysis of the strains in (A). GerAA(WT) and GerAA(V362A) were expressed at similar levels in the presence or absence of GerAB and GerAC. ScpB controls for loading.

(C) Representative fluorescence images of exponentially growing cultures of the indicated strains from (A). Time (in minutes) after IPTG addition is indicated. The top panels show fluorescence of the potentiometric dye DiSC₃(5). The lower panels show propidium iodide staining. The two fields are from the same culture but stained and imaged separately. Scale bar, 5 μm. (D) Representative DiSC₃(5) fluorescence images of exponentially growing cultures of the indicated strains 30 min after the addition of 50 mM L-alanine. *gerAA* and *gerAA*(V362L) are IPTG-regulated alleles, and *gerAB*, *gerAB*(G25A), and *gerAC* were expressed constitutively. (E) Quantitative analysis of DiSC₃(5) fluorescence intensity from the same strains and conditions as in (D). DiSC₃(5) fluorescence intensities were quantified from three biological replicates (>500 cells for each) and plotted in different colors. Triangles represent the median fluorescence intensity for each replicate, and red lines show the median values for all cells per strain. *P* values < 0.0001 (****) and not significant (ns) are indicated.

(F) Immunoblots of anti-ProC immuno-affinity purifications from detergent-solubilized membrane preparations of vegetatively growing *B. subtilis* cells expressing the indicated proteins. Load (L) and elution (Elu) are shown. GerAA-FLAG copurifies with GerAA-ProC if GerAB and GerAC are coexpressed. The membrane protein EzrA serves as a negative control. (G) Representative fluorescence images of vegetative cells expressing GerAA-GFP in the presence and absence of GerAB and GerAC. (H) Immunoblots of vegetative cells expressing cysteine-substituted GerAA variants in the presence or absence of GerAB and GerAC. GerAA(V359C G361C) produces disulfide species (red asterisks) with sizes of dimer and pentamer (left). Wall controls were used for loading. GerAA species of similar size were also detected from spore lysates (right). Two additional species were detected. SleB controls were used for loading. Representative data from one of at least three biological replicates are shown for (A), (C) to (E), (G), and (H). (B) and (F) are from one of two biological replicates.

(A) Serial dilutions of the indicated strains with IPTG-regulated *gerAA*(WT) and *gerAA*(V362A) alleles and constitutively expressed *gerAB* and *gerAC* (AC). (B) Immunoblot analysis of the strains in (A). GerAA(WT) and GerAA(V362A) were expressed at similar levels in the presence or absence of GerAB and GerAC. ScpB controls for loading.



Discussion

Our data support a model in which L-alanine detection by GerAB subunits in the GerA complex acts cooperatively to induce a conformational change in the GerAA subunits, which in turn opens the transmembrane channel and allows cation release. That the *B. subtilis* GerA receptor can trigger DPA expulsion by the *B. cereus* and *C. difficile* SpoVA transporters and, reciprocally, that the *B. megaterium* GerUV

receptor can trigger DPA export by *B. subtilis* SpoVA further suggest that ion release by GerA-family receptors activates the SpoVA complex and ultimately spore germination.

An Na⁺/H⁺-K⁺ antiporter in *B. cereus*, GerN, is required for spore germination in response to inosine (33). *B. cereus* spores lacking *gerN* are impaired in ion release and subsequent germination when exposed to inosine but respond normally to L-alanine. GerN is not broadly

conserved among spore formers and is absent in *B. subtilis* (33). Furthermore, no ion transporters have been found in *B. cereus* that are required for spores to respond to L-alanine (34), and analysis of remote homologs of GerN and other putative ion transporters present in the *B. subtilis* spore inner membrane have failed to identify analogous transporters required for germination (14) (fig. S26). Nonetheless, the studies on *B. cereus* GerN provide

foundational evidence that cation release is required in the germination signal transduction pathway. The data presented here are consistent with these studies and suggest that the link between ion release and germination is not the exception but rather the rule. Indeed, our work suggests that in most cases, GerA-family complexes function as the principal germination-initiating ion channels.

Our finding that GerA receptors are ligand-gated ion channels provides a mechanistic explanation for how a transient pulse of L-alanine could trigger a pulse of K⁺ release, as was recently proposed to explain how spores retain the memory of a previous exposure to nutrients (35). In this model, germination is only triggered when the intracellular K⁺ concentration drops below a threshold value and each transient exposure to nutrients incrementally reduces ion concentration until this threshold is reached. Although we favor the idea that the SpoVA transport complex is activated to release DPA when intracellular K⁺ concentrations drop below a threshold value, the memory model proposed by Süel and co-workers (35) cannot account for previous observations that the memory of an exposure to nutrients is lost over time (36, 37). This short-term memory can, however, be explained by the requirement for L-alanine to bind multiple, if not all, GerAB subunits in the pentameric complex to trigger ion release. If a transient pulse of L-alanine results in partial occupancy and dissociation is slow, then the subsequent pulse could more readily achieve full occupancy and open the GerAA channel. This model is consistent with the different rates of memory loss observed for different nutrient stimuli and the faster memory loss when spores are incubated at high temperature between germinant pulses (36).

It is noteworthy that ~4.2% of all sequenced germinant receptor operons encode two or more B subunits in addition to single A and C subunits (8). In the case of the *B. megaterium gerUV* locus, the two B subunits (GerUB and GerVB) can each function without the other, provided that their shared A and C subunits are present (13). These data suggest that different B subunits could assemble into a single

pentameric receptor. Because B subunits function in nutrient detection, these mixed pentamers could integrate distinct nutrient signals in the environment.

In summary, our data indicate that GerA-family receptors assemble into a family of pentameric ligand-gated ion channels that transduce germinant signals by releasing cations, which activates SpoVA complexes to expel DPA from the spore core. DPA release triggers degradation of the spore cortex peptidoglycan and exit from dormancy.

REFERENCES AND NOTES

1. S. André, T. Vallaeys, S. Planchon, *Res. Microbiol.* **168**, 379–387 (2017).
2. M. Mallozzi, V. K. Viswanathan, G. Vedantam, *Future Microbiol.* **5**, 1109–1123 (2010).
3. P. Setlow, *Microbiol. Spectr.* **2**, 2.5.11 (2014).
4. A. Moir, G. Cooper, *Microbiol. Spectr.* **3**, microbiolspec.TBS-0014-2012 (2015).
5. P. Setlow, S. Wang, Y. Q. Li, *Annu. Rev. Microbiol.* **71**, 459–477 (2017).
6. Y. Gao *et al.*, *Genes Dev.* **36**, 634–646 (2022).
7. V. R. Vepachedu, P. Setlow, *J. Bacteriol.* **189**, 1565–1572 (2007).
8. D. Paredes-Sabja, P. Setlow, M. R. Sarker, *Trends Microbiol.* **19**, 85–94 (2011).
9. J. D. Amon, L. Artzi, D. Z. Rudner, *J. Bacteriol.* **204**, e0047021 (2022).
10. L. Artzi *et al.*, *Nat. Commun.* **12**, 6842 (2021).
11. J. Trowsdale, D. A. Smith, *J. Bacteriol.* **123**, 83–95 (1975).
12. M. B. Francis, C. A. Allen, R. Shrestha, J. A. Sorg, *PLoS Pathog.* **9**, e1003356 (2013).
13. G. Christie, C. R. Lowe, *J. Bacteriol.* **189**, 4375–4383 (2007).
14. Y. Chen *et al.*, *J. Bacteriol.* **201**, e0062-18 (2019).
15. B. M. Sverdlow, B. Setlow, P. Setlow, *J. Bacteriol.* **148**, 20–29 (1981).
16. R. B. Bass, P. Strop, M. Barclay, D. C. Rees, *Science* **298**, 1582–1587 (2002).
17. R. Evans *et al.*, *bioRxiv*, 2021.2010.2004.463034 (2022).
18. J. Jumper *et al.*, *Nature* **596**, 583–589 (2021).
19. M. Mirdita *et al.*, *Nat. Methods* **19**, 679–682 (2022).
20. T. A. Hopf *et al.*, *Bioinformatics* **35**, 1582–1584 (2019).
21. Á. Nemezc, M. S. Prevost, A. Menny, P. J. Corringier, *Neuron* **90**, 452–470 (2016).
22. S. Uysal *et al.*, *Proc. Natl. Acad. Sci. U.S.A.* **106**, 6644–6649 (2009).
23. N. Unwin, *J. Mol. Biol.* **346**, 967–989 (2005).
24. S. Zhu *et al.*, *Nature* **559**, 67–72 (2018).
25. W. Mongkolkeha, G. R. Cooper, J. S. Mawer, R. N. Allan, A. Moir, *J. Bacteriol.* **193**, 2268–2275 (2011).
26. K. K. Griffiths, J. Zhang, A. E. Cowan, J. Yu, P. Setlow, *Mol. Microbiol.* **81**, 1061–1077 (2011).
27. P. J. Barlass, C. W. Houston, M. O. Clements, A. Moir, *Microbiology (Reading)* **148**, 2089–2095 (2002).
28. J. A. Maurer, D. E. Elmore, H. A. Lester, D. A. Dougherty, *J. Biol. Chem.* **275**, 22238–22244 (2000).

29. X. Ou, P. Blount, R. J. Hoffman, C. Kung, *Proc. Natl. Acad. Sci. U.S.A.* **95**, 11471–11475 (1998).
30. J. D. te Winkel, D. A. Gray, K. H. Seistrup, L. W. Hamoen, H. Strahl, *Front. Cell Dev. Biol.* **4**, 29 (2016).
31. C. R. Woese, H. J. Morowitz, C. A. Hutchison3rd, *J. Bacteriol.* **76**, 578–588 (1958).
32. T. L. Kirtley, *J. Biol. Chem.* **265**, 4227–4232 (1990).
33. P. D. Thackray, J. Behravan, T. W. Southworth, A. Moir, *J. Bacteriol.* **183**, 476–482 (2001).
34. A. Senior, A. Moir, *J. Bacteriol.* **190**, 6148–6152 (2008).
35. K. Kikuchi *et al.*, *Science* **378**, 43–49 (2022).
36. S. Wang, J. R. Faeder, P. Setlow, Y. Q. Li, *mBio* **6**, e01859–e15 (2015).
37. P. Zhang, J. Liang, X. Yi, P. Setlow, Y. Q. Li, *J. Bacteriol.* **196**, 2443–2454 (2014).
38. M. J. Wilson, P. E. Carlson, B. K. Janes, P. C. Hanna, *J. Bacteriol.* **194**, 1369–1377 (2012).

ACKNOWLEDGMENTS

We thank I. Shlosman, A. Alon, and all members of the Bernhardt-Rudner supergroup for helpful advice, discussions, and encouragement; A. Vettiger and the HMS Microscopy Resources on the North Quad (MicRoN) core for advice on microscopy and analysis; and the Center for Environmental Health Sciences Bioanalytical Core Facility at MIT, for access to its ICP-MS. All three co-first authors made foundational discoveries and contributed equally to this work. L.A. formulated the key hypothesis that GerAA could multimerize into an ion channel. Portions of this research were conducted on the O2 High Performance Computing Cluster, which is supported by the Research Computing Group at Harvard Medical School. **Funding:** This work was supported by the National Institutes of Health (grants GM086466, GM127399, GM122512, and AI171308 to D.Z.R.; grant AI164647 to D.Z.R., A.C.K., and D.S.M.; and grant F32GM130003 to J.D.A.) and by funds from the Harvard Medical School Dean's Initiative. L.A. was a Simons Foundation fellow of the Life Sciences Research Foundation. **Author contributions:** Conceptualization: L.A., J.D.A., Y.G., A.C.K., D.Z.R.; Investigation: L.A., J.D.A., Y.G., F.H.R.-G., J.C.C.; Resources: K.P.B., D.S.M.; Supervision: D.Z.R., A.C.K.; Writing – original draft: L.A., J.D.A., Y.G., F.H.R.-G., D.Z.R.; Writing – review & editing: K.P.B., J.C.C., D.S.M., A.C.K. **Competing interests:** D.S.M. is a cofounder of Seismic Therapeutics and an adviser for Dyno Therapeutics, Octant, Jura Bio, Tectonic Therapeutics, and Genentech. The remaining authors declare no competing interests. **Data and materials availability:** All data are available in the manuscript or the supplementary materials. **License information:** Copyright © 2023 the authors, some rights reserved; exclusive licensee American Association for the Advancement of Science. No claim to original US government works. <https://www.science.org/about/science-licenses-journal-article-reuse>

SUPPLEMENTARY MATERIALS

[science.org/doi/10.1126/science.adg9829](https://doi.org/10.1126/science.adg9829)

Materials and Methods

Figs. S1 to S26

Tables S1 to S3

References (39–63)

Data S1 to S5

MDAR Reproducibility Checklist

[View/request a protocol for this paper from Bio-protocol.](#)

Submitted 3 February 2023; accepted 29 March 2023
10.1126/science.adg9829



Bacterial spore germination receptors are nutrient-gated ion channels

Yongqiang Gao, Jeremy D. Amon, Lior Artzi, Fernando H. Ramirez-Guadiana, Kelly P. Brock, Joshua C. Cofsky, Deborah S. Marks, Andrew C. Kruse, and David Z. Rudner

Science, **380** (6643), .

DOI: 10.1126/science.adg9829

Editor's summary

Bacterial spores are able to resist heat, desiccation, irradiation, organic solvents, and antibiotics and can remain metabolically inactive for decades. Nevertheless, an encounter with nutrients triggers exit from dormancy and resumption of growth within minutes. How these inert bodies monitor their environment and trigger germination remains unclear. Working with the bacterium *Bacillus subtilis*, Gao *et al.* found that germinant receptors embedded in the spore membrane oligomerize into nutrient-gated ion channels and then ion release triggers exit from dormancy. Future studies could lead to treatments that induce germination, leaving pathogens vulnerable to antibiotics, or that block exit from dormancy, directly preventing disease. —Stella M. Hurtley

View the article online

<https://www.science.org/doi/10.1126/science.adg9829>

Permissions

<https://www.science.org/help/reprints-and-permissions>

Use of this article is subject to the [Terms of service](#)

Science (ISSN) is published by the American Association for the Advancement of Science. 1200 New York Avenue NW, Washington, DC 20005. The title *Science* is a registered trademark of AAAS.

Copyright © 2023 The Authors, some rights reserved; exclusive licensee American Association for the Advancement of Science. No claim to original U.S. Government Works